ELSEVIER

Nuclear Physics A 686 (2001) 129–140

NUCLEAR PHYSICS A

www.elsevier.nl/locate/npe

Band crossing and signature splitting in odd mass fp shell nuclei

Victor Velázquez [a], Jorge G. Hirsch [b,*], Yang Sun [c,d]

[a] *Institute de Recherches Subatomiques (IN2P3-CNRS-Université Louis Pasteur), Bâtiment 27/1, F-67037 Strasbourg cedex 2, France*

[b] *Instituto de Ciencias Nucleares, Universidad Nacional Autónoma de México, Circuito Exterior C.U., AP 70-543, 04510 México DF, México*

[c] *Department of Physics and Astronomy, University of Tennessee, Knoxville TN, 37996, USA*

[d] *Department of Physics, Xuzhou Normal University, Xuzhou, Jiangsu 221009, PR China*

Received 10 May 2000; revised 25 September 2000; accepted 12 October 2000

Abstract

Structure of two sets of mirror nuclei: ^{47}V–^{47}Cr and ^{49}Cr–^{49}Mn, as well as ^{49}V and ^{51}Mn, is studied using the projected shell model. Their yrast spectra are described as an interplay between the angular momentum projected states around the Fermi level which carry different intrinsic K-quantum numbers. The deviations from a regular rotational sequence are attributed to band crossing and signature splitting, which are usually discussed in heavy nuclear systems. Our results agree reasonably with experimental data, and are comparable with those from the full pf shell model calculations.

PACS: 21.10.Re; 21.60.Cs; 23.20.Lv; 27.40.+z

Keywords: Projected shell model; Rotational band; Backbending; Energy staggering; Band crossing; Signature splitting

1. Introduction

Our knowledge about the nuclear structure around ^{48}Cr has been improved enormously in recent years. Multielement gamma-ray detectors have allowed the establishment of rotational structures in ^{46,47}Ti, ^{47,48}V, and ^{47,48,49,50}Cr, with clear evidence of backbending found in ^{48,50}Cr [1–5]. These experiments have been performed in a close interaction with the full *pf* shell model calculations, which have provided us with a nearly perfect description of the rotational bands in many of these nuclei [6–9].

* Corresponding author.
E-mail address: hirsch@nuclecu.unam.mx (J.G. Hirsch).

0375-9474/01/$ – see front matter
PII: S0375-9474(00)00507-8

While the backbending mechanism in heavy nuclei is commonly understood as a band crossing phenomenon involving two rotational bands with different moments of inertia [10], the origin of backbending in ^{48,50}Cr at spin $I \approx 10$ has been debated. Caurier et al. [7] provided exact solutions of the Hamiltonian within the complete *pf* shell. The backbending effect was attributed to a collective to noncollective transition. Later, Martínez-Pinedo et al. [8] performed a similar study for ^{50}Cr, in which they reproduced the first backbending, and predicted a second backbending at $I = 18$ which was confirmed experimentally one year later [4]. Using a self-consistent cranked Hartree–Fock–Bogoliubov formalism, Tanaka et al. offered an explanation for the backbending in ^{48}Cr, in which they proposed that the phenomenon is not associated with a single-particle level crossing [11].

In a recent paper by Hara et al. [12], the backbending mechanism of ^{48}Cr was studied within the projected shell model (PSM) [13], which has been successful in describing well deformed heavy nuclei [13] and those of transitional region [14]. In [12], it was concluded that the backbending in ^{48}Cr is due to a band crossing involving an excited band built on simultaneously broken pairs of neutrons and protons in the "intruder" subshell $f_{7/2}$. This type of band crossing is usually known to cause a second backbending in rare-earth nuclei. In the same work [12], it was shown, by using the generator coordinate method (GCM) with the same Hamiltonian as that of the pf shell model calculation, that the backbending in ^{48}Cr can be interpreted as due to the crossing between the deformed and spherical bands. Detailed analysis indicated that the two theories (PSM and GCM) lead to a consistent picture of band crossing since the physical content of the 4-qp band in PSM and that of the spherical band in GCM is very similar [12].

The purpose of the present paper is to demonstrate that the PSM is not only able to explain the backbending phenomenon in the even–even nucleus ^{48}Cr, but it can, using the same set of parameters, describe the odd-mass nuclei ^{47,49}V,^{47,49}Cr and ^{49,51}Mn. These nuclei have been extensively studied with the full pf shell diagonalizations [9]. It will be seen here that the band crossing mechanism also explains the deviation from a regular sequence for rotational bands in some of these odd-mass nuclei. Furthermore, the observed energy staggering along a band can be well described by the PSM in terms of the signature splitting, a terminology that originates from the particle-rotor model.

The paper is arranged as follows: in Section 2, we outline the PSM and present the Hamiltonian and the model space used in our calculation. Detail discussion on the structure of these nuclei and comparison with experimental data are given in Section 3. Finally, we summarize our paper in Section 4.

2. Outline of the theory

The use of a deformed basis allows construction of an optimal set of basis states, in which shell model truncation can be done most efficiently by selecting the low-lying configurations around the Fermi level [13]. It provides a good classification scheme in the sense that a simple configuration corresponds (approximately) to a low excitation

mode of the nucleus. To carry out a shell model type calculation with such a deformed basis, the broken rotational symmetry (and the particle-number conservation if necessary) has to be restored. Projection generates a new basis in the laboratory frame in which the Hamiltonian is diagonalized. Thus, the final diagonalization is carried out in a space with a very small size (usually in a dimension smaller than 100), which has a well-defined microscopic structure and allows a physical interpretation in terms of rotational bands and the interaction between them.

Quasiparticles defined in the deformed Nilsson + BCS calculations are the starting point of the PSM. The set of multi-qp states for our shell model configuration space is

$$|\Phi_\kappa\rangle = \left\{a_\nu^\dagger|0\rangle,\ a_\nu^\dagger a_{\pi_1}^\dagger a_{\pi_2}^\dagger|0\rangle\right\}, \tag{1}$$

for odd-neutron nuclei, and

$$|\Phi_\kappa\rangle = \left\{a_\pi^\dagger|0\rangle,\ a_\pi^\dagger a_{\nu_1}^\dagger a_{\nu_2}^\dagger|0\rangle\right\}, \tag{2}$$

for odd-proton nuclei, where $a^\dagger$'s are the quasiparticle (qp) creation operators, ν's (π's) denote the neutron (proton) Nilsson quantum numbers which run over low-lying orbitals and $|0\rangle$ is the Nilsson + BCS vacuum (0-qp state). In Eqs. (1) and (2), the low-lying 3-qp states selected for the many-body basis are those consisting of 1-qp plus a pair of qp's from nucleons of another kind. This selection is based on physical considerations. In general, 3-qp states made by three nucleons of the same kind are also allowed, but such states usually lie higher in energy.

The PSM employs the Hamiltonian [13]

$$\widehat{H} = \widehat{H}_0 - \frac{1}{2}\chi\sum_\mu \widehat{Q}_\mu^\dagger\widehat{Q}_\mu - G_{\rm M}\widehat{P}^\dagger\widehat{P} - G_{\rm Q}\sum_\mu \widehat{P}_\mu^\dagger\widehat{P}_\mu. \tag{3}$$

It contains the spherical single-particle term $\widehat{H}_0$ which includes a proper spin–orbit force taken from Ref. [15], the Q–Q interaction (the second term), and the monopole and quadrupole pairing interactions (the last two terms). They represent the most important correlations in nuclei [16]. The Q–Q interaction strength χ is adjusted by the self-consistent relation between the quadrupole deformation ε_2 and the one resulting from the HFB procedure [13,17]. The monopole pairing strength $G_{\rm M}$ is taken to be $G_{\rm M} = [g_1 \mp g_2(N-Z)/A]/A$, where $g_1 = 22.5$ and $g_2 = 18.0$, and $-(+)$ is for protons (neutrons). These are the appropriate values when three major shells ($N = 1, 2, 3$) are included in the single-particle space [12]. The quadrupole pairing strength $G_{\rm Q}$ is assumed to be proportional to $G_{\rm M}$, with a proportionality constant taken in the range of 0.16–0.20.

For each spin I the set of eigenvalue equations in the PSM are [13]

$$\sum_{\kappa'}\left\{H^I_{\kappa\kappa'} - E^{I\alpha}N^I_{\kappa\kappa'}\right\}F^{I\alpha}_{\kappa'} = 0, \tag{4}$$

with α denoting states having a same spin I. The Hamiltonian matrix elements $H^I_{\kappa\kappa'}$ and the norm matrix elements $N^I_{\kappa\kappa'}$ are defined as

$$H^I_{\kappa\kappa'} = \langle\Phi_\kappa|\widehat{H}\widehat{P}^I_{KK'}|\Phi_{\kappa'}\rangle, \qquad N^I_{\kappa\kappa'} = \langle\Phi_\kappa|\widehat{P}^I_{KK'}|\Phi_{\kappa'}\rangle, \tag{5}$$

where $\widehat{P}^I_{MK}$ is the angular momentum projection operator.

The band energy is defined as the expectation value of the Hamiltonian with respect to a "rotational band κ" $H^I_{\kappa\kappa}/N^I_{\kappa\kappa}$, which are the diagonal elements in Eq. (5). A band diagram is a plot of the band energies as functions of spin I. It provide a useful tool for interpreting the results [13].

Signature is a quantum number specifically appearing in a deformed intrinsic system [18]. For an odd-A nucleus, it is customary to assign

$$\alpha_I = \tfrac{1}{2}(-1)^{I-1/2} \tag{6}$$

as the signature quantum number for a state of spin I. Thus, a rotational band with a sequence of levels differing in spin by 1 is now divided into two branches, each consisting of levels differing in spin by 2 and classified by the signature quantum number $\alpha_I = \pm\frac{1}{2}$, respectively. Experimentally, one often observes an energy staggering in rotational bands and refers to this as signature splitting [19]. The favored band is the branch that is pushed down in energy, while the unfavored band is the one that is pushed up.

As an observable phenomenon, splitting of one band into two branches should manifest itself in any nuclear many-body theory. In fact, the pf shell model diagonalization for $A = 47$ and 49 nuclei [9] has correctly reproduced the energy staggerings in the rotational bands. The PSM description of the signature splitting has been extensively studied by Sun et al. [20].

3. Structure of the odd-mass nuclei

In the present work, we study the odd-mass pf shell nuclei by applying the PSM in two sets of mirror nuclei: ^{47}V–^{47}Cr and ^{49}Cr–^{49}Mn, which are odd-mass nuclei relative to the even–even ^{48}Cr with either adding or removing one particle. In addition, we study another two odd-mass nuclei ^{49}V and ^{51}Mn.

Given that these odd-mass nuclei are reasonably good rotors at least at low spins [9], we fix the same quadrupole deformation $\epsilon = 0.25$ in the deformed basis for all nuclei studied in this paper, which is the same value used in ^{48}Cr [12]. We use also the same monopole and quadrupole pairing strength constants employed in the previous PSM calculations [12].

In Fig. 1, we present the energy spectra of these six nuclei. Comparison is made between the experimental data [21] shown at the left hand side, and the PSM results at the right hand side. Fig. 2 contains the energy difference $E(I) - E(I-1)$ (in MeV) versus spin I plots. The solid lines represent the experimental data and the dashed lines the PSM results. Fig. 3 shows the band diagrams $H^I_{\kappa\kappa}/N^I_{\kappa\kappa}$ versus spin I, with solid lines representing 1-qp bands, dashed lines 3-qp bands, and the diamonds the yrast band obtained from the PSM diagonalization (experimental results are not shown in this figure). In Fig. 3, although more low-lying bands have been included in the calculation, we display only the most important bands to illustrate the physics. Theoretical energies of the yrast bands in Fig. 3 are those used in Figs. 1 and 2 to compare with data.

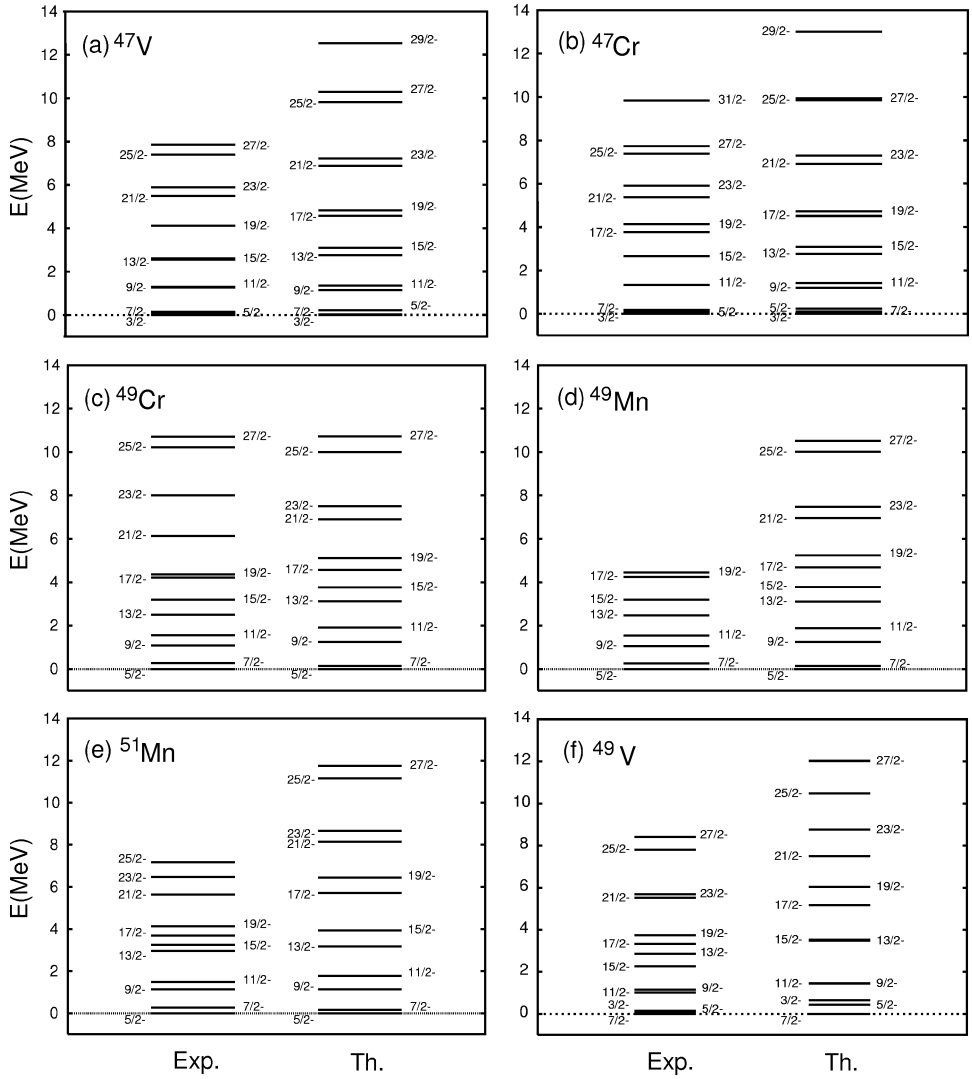

Fig. 1. Energy levels of ^{47}V, ^{47}Cr, ^{49}Cr, ^{49}Mn, ^{51}Mn and ^{49}V are shown in inserts (a)–(f), respectively. Experimental levels are presented in the left-hand side and the PSM results at right-hand side.

3.1. ^{47}V–^{47}Cr

The pair of mirror nuclei ^{47}V–^{47}Cr has been studied within the *pf* shell model [9], motivating new experimental work in this mass region [3]. These two sets of data look very similar, characterized by a nearly degenerate energy triplet near the ground state and several doublets above it, indicating strong energy staggerings in the yrast bands.

Figs. 1a and 1b present the energy levels of ^{47}V and ^{47}Cr, respectively. The correct ground-state spin and parity $\frac{3}{2}^-$ are found for both nuclei. The almost degenerate ground-

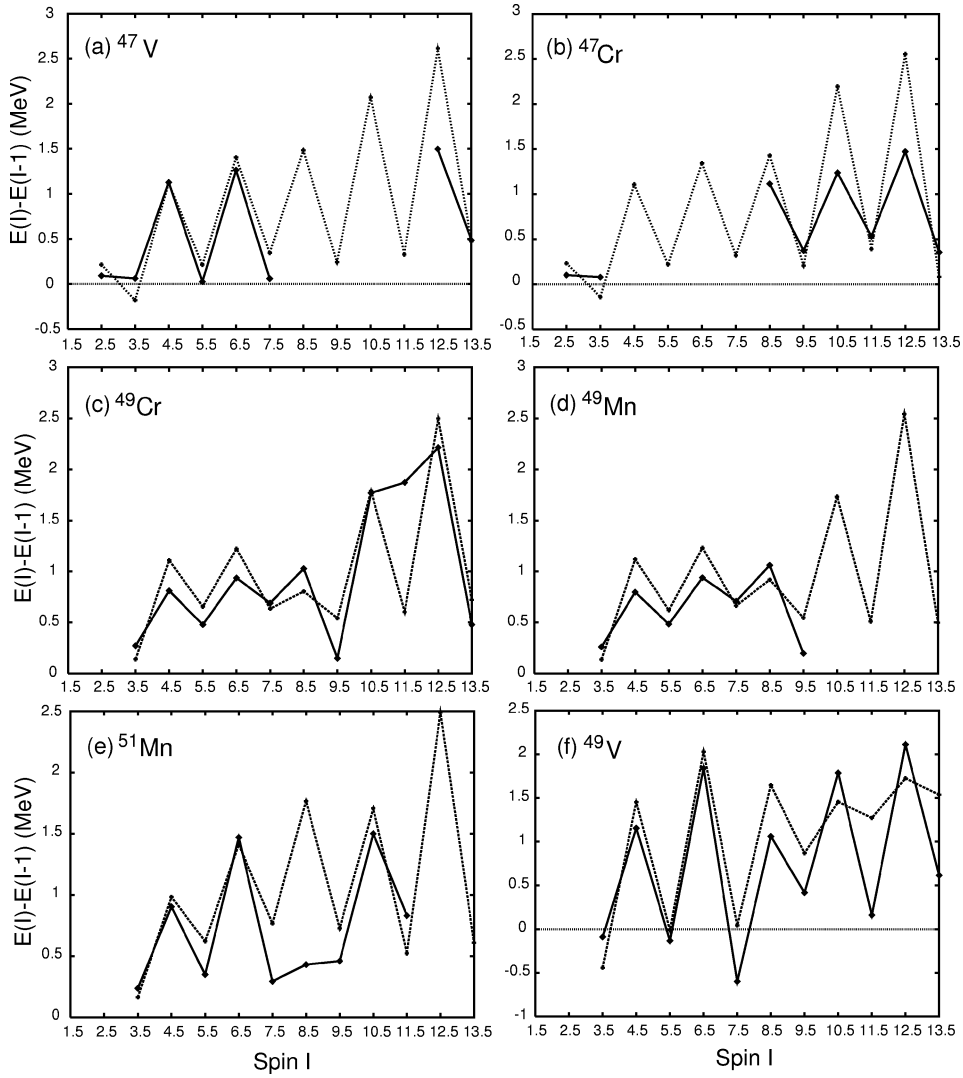

Fig. 2. $E(I) - E(I-1)$ vs. I curves with the same order of Fig. 1. The experimental values are plotted in solid lines with diamonds, the PSM calculations in dashed lines with crosses.

state triplet $\left[\frac{3}{2}^-, \frac{5}{2}^-, \frac{7}{2}^-\right]$ is clearly reproduced. However, for ^{47}Cr, the theory predicts an inversion between the first $\frac{5}{2}^-$ and $\frac{7}{2}^-$ states which is not found in the experiment. The PSM description of the spectra is quite good, but the predicted moments of inertia are smaller than the experimental ones. It can be clearly seen that for energies higher than 6 MeV, the predicted states are displaced at higher energies compared to the experiment. Given that the Nilsson single-particle energies do not show crossings in this region around $\epsilon = 0.25$, we do not expect that increasing the mean field deformation will modify the moment of inertia very much. Nevertheless, it is remarkable that the conceptually and

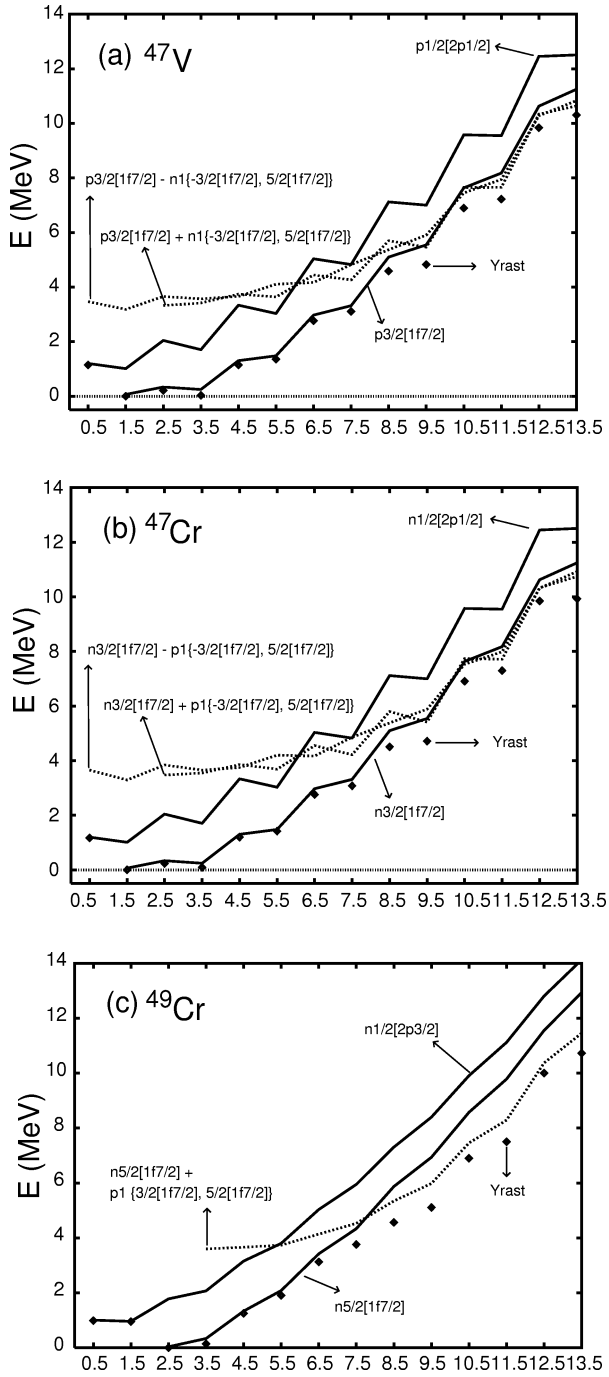

Fig. 3. Band diagrams E vs. I with the same order of Fig. 1. The yrast band is represented with diamonds, the 1-qp bands with solid lines and the 3-qp bands with dashed lines.

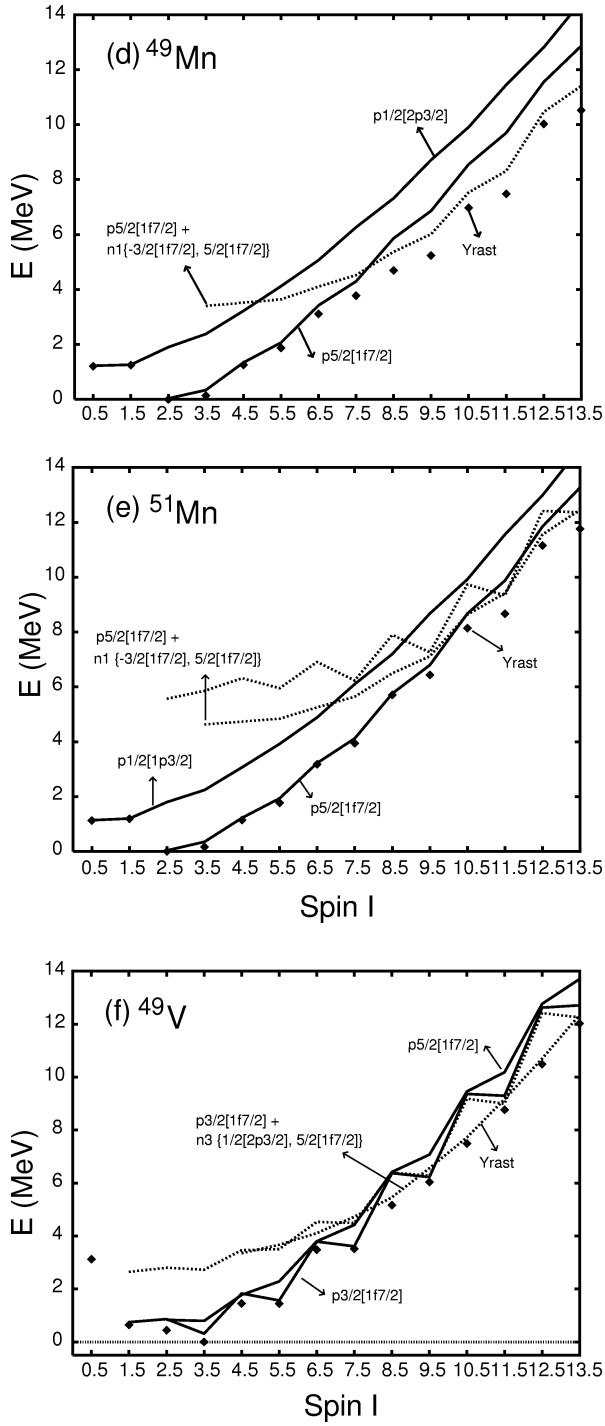

Fig. 3. —continued.

numerically simple PSM results are competitive with those found in the full *pf* shell model diagonalizations [9], which reproduced the overall energy scale very well, but predicted a couple of doublets inverted.

As can be seen in Fig. 2a, the observed energy staggering is well reproduced in ^{47}V. Similar staggering is predicted for ^{47}Cr in Fig. 2b, for which the existing data at low spins are not sufficient to make a comparison. In both cases, the first two energy differences are exaggerated by the model.

We now discuss the band diagram in Fig. 3 to understand the physics. In Fig. 3a, we see that the low-spin states of the yrast band in ^{47}V are dominated by the proton $K = \frac{3}{2}$ state in $1f_{7/2}$ orbit. For ^{47}Cr, the yrast band at low spins is mainly the band corresponding to the neutron $K = \frac{3}{2}$ state in $1f_{7/2}$ orbit. Bands lying higher in energy have negligibly small influence in the mixing to the $K = \frac{3}{2}$ one, as we can see that the filled diamonds take the value of the $K = \frac{3}{2}$ band almost exactly. The staggering in both yrast bands is such that the spin sequence of $I = \frac{3}{2}, \frac{7}{2}, \ldots$ is pushed down in energy. Note that the physics is almost entirely described by projection onto the intrinsic $K = \frac{3}{2}$ state. The correct staggering phase and amplitude along the bands are obtained by the PSM quantum mechanical treatment.

We thus understand why the experimentally observed energy doublets and triplets can happen in these nuclei. Near the band head, the small splitting effect pushes the $I = \frac{7}{2}$ state close to the $I = \frac{3}{2}$ and $I = \frac{5}{2}$ states, forming a nearly degenerate energy triplet. Above them, states belonging to the $I = \frac{3}{2}$ branch are pushed down to be close to the signature partners in the $I = \frac{5}{2}$ branch, so that the energy doublets are formed. In the ^{47}V data, the energy difference between the states of $I = \frac{9}{2}$ and $I = \frac{11}{2}$, and of $I = \frac{13}{2}$ and $I = \frac{15}{2}$, is close to zero, indicating an almost perfect degeneration. We notice that in the measured data of ^{47}V and ^{47}Cr, for several predicted degenerate doublets, only one state of the two signature partners has been observed.

Data of the ^{47}V and ^{47}Cr nuclei seem to suggest that there is no band crossing at low-spin states. From Figs. 3a and 3b we see that, in both nuclei, there is a band crossing near $I = \frac{19}{2}$ between the 1-qp $K = \frac{3}{2}$ band (lower solid line) and the 3-qp bands (dashed lines). However, the band crossing in ^{47}Cr occurs in higher energy without involving the lowest lying $K = \frac{3}{2}[1f_{7/2}]$ band. In ^{47}V, the 3-qp bands cross the $K = \frac{3}{2}[1f_{7/2}]$ band with only a small crossing angle so that the yrast band changes smoothly its structure from the 1-qp to the 3-qp states. Therefore, in both cases, no sizable effect from the band crossing can be observed in the energy spectra. This is in contrast to the situation in ^{49}Cr and ^{49}Mn nuclei, as we shall discuss below.

3.2. ^{49}Cr–^{49}Mn

The second pair of mirror nuclei studied in this paper is ^{49}Cr–^{49}Mn. For these two nuclei, the ground-state spin and parity are $\frac{5}{2}^-$. The separation of the energy doublets is generally larger, and the degeneracy is not as good as in ^{47}V–^{47}Cr. In other words, the staggering amplitude is smaller at the low-spin states. Another notable differences from ^{47}V–^{47}Cr are

the irregularities clearly seen in the spectra around the state $I = \frac{17}{2}$. The structure of this pair of nuclei have also been extensively discussed within the *pf* shell model [9].

The energy spectra shown in Figs. 1c and 1d agree well with the experimental data. In particular, the doublet $\left[\frac{25}{2}^-, \frac{27}{2}^-\right]$ in ^{49}Cr is predicted at energies above 10 MeV, well reproducing the experimental energies reported in the compilation of experimental data [21]. The irregular staggering in these two nuclei can be seen in Figs. 2c and 2d. The PSM reproduces fairly well the changes in energy differences, which is more evident for ^{49}Cr where there are more data available.

From Figs. 3c and 3d, we can see that in both nuclei, the yrast band is dominated by a $K = \frac{5}{2}$ 1-qp band up to $I = \frac{15}{2}$. Since these are higher K-bands, the staggering is weaker than what we have seen for the $K = \frac{3}{2}$ bands in Figs. 3a and 3b. This explains why the level separation of the energy doublets is generally larger in these two nuclei, as seen in Fig. 1.

Around $I = \frac{17}{2}$, a 3-qp band crosses sharply the $K = \frac{5}{2}$ 1-qp band in both cases. This sharp crossing disturbs suddenly the regular band and changes components in the wave function. After the band crossing, the yrast bands are mainly 3-qp states. The 3-qp states in ^{49}Cr and ^{49}Mn have also mirror configurations. In ^{49}Cr, it consists of the neutron $\frac{5}{2}[1f_{7/2}]$ plus a proton pair $K = 1\left\{\frac{3}{2}[1f_{7/2}], \frac{5}{2}[1f_{7/2}]\right\}$, whereas in ^{49}Mn, the structure is the proton $\frac{5}{2}[1f_{7/2}]$ plus a neutron pair $K = 1\left\{\frac{3}{2}[f_{7/2}], \frac{5}{2}[1f_{7/2}]\right\}$. Neglecting the effect of isospin symmetry breaking, we thus expect the spectra of these two nuclei to be similar.

Influence of the band crossing around $I = \frac{17}{2}$ in this pair of nuclei can be seen in Figs. 2c and 2d. The staggering changes in amplitude as function of spin are correctly reproduced, although there are visible deviations.

3.3. ^{51}Mn and ^{49}V

As an isotope of ^{49}Mn, we expect a similar behavior of the lowest proton 1-qp state in ^{51}Mn. One may also expect to see differences around the band crossing region, where two additional neutrons are involved in the 3-qp states. Due to shift of the neutron Fermi levels in the two nuclei ^{49}Mn and ^{51}Mn, behavior of the 3-qp bands can be different, which can leave the energy spectra around the band crossing regions different.

The energy spectra of ^{51}Mn and ^{49}V are shown in Figs. 1e and 1f. As in the $A = 47$ case, the ordering of the states as well as the ground-state spin are well reproduced. As shown in Fig. 2e, the PSM reproduces the energy differences with correct phases and amplitudes for the most measured states in ^{51}Mn, but fails to reproduce the sudden reduction of the $E(I) - E(I-1)$ value at spin $I = \frac{19}{2}$. The reason for this discrepancy can be seen in Fig. 3e, where the position of the 3-qp band is too high in energy, and thus crosses the 1-qp $K = \frac{5}{2}$ band gently at a too late spin state.

In Fig. 2f, the staggering in ^{49}V is successfully described by the PSM up to $I = \frac{19}{2}$. For larger-spin states the PSM underestimates the changes in energy differences. This discrepancy, as can be seen in Fig. 3f, has its origin in the fact that the 3-qp state consisting of the proton $\frac{3}{2}[1f_{7/2}]$ plus the neutron pair $K = 3\left\{\frac{1}{2}[2p_{3/2}], \frac{5}{2}[1f_{7/2}]\right\}$ dives into the yrast

region after the band crossing. This is a high-K band, thus has a very weak staggering effect, according to our early discussions.

There is an interesting observation that is worth to be pointed out. As an isotope of ^{47}V, we expect that the 1-qp proton state $\frac{3}{2}[1f_{7/2}]$ dominates the low-spin states in the yrast band of ^{49}V also, and that similar triplet states should be observed around the ground state. Indeed, such a nearly degenerate triplet has been seen experimentally as shown in Fig. 1f, but the order of these states are reversed as $\left[\frac{7}{2}^-, \frac{5}{2}^-, \frac{3}{2}^-\right]$. It is seemingly anomalous that this nucleus has the ground-state spin $I = \frac{7}{2}$, but the corresponding intrinsic state has $K = \frac{3}{2}$. The physical reason for this anomaly can be understood as the interaction of the 1-qp proton $\frac{3}{2}[1f_{7/2}]$ band with the 1-qp proton $\frac{5}{2}[1f_{7/2}]$ band which lies just little above the former. As the consequence of the interaction, the yrast states of $I = \frac{5}{2}$ and $\frac{7}{2}$ are pushed down in energy, and become lower than the $I = \frac{3}{2}$ state which should otherwise be the ground state as in the ^{47}V case. This feature has been described correctly by the PSM.

4. Summary

The present results confirm that the PSM is a practical tool in studying rotational bands, which, having been successful in describing deformed and triaxial rare earth nuclei, is also able to provide a quantitative and simple description of light nuclei. In a previous work, the backbending of ^{48}Cr was described using the PSM as a band crossing phenomena found in heavier nuclei. The same ideas have proved fruitful here to describe the irregularities in rotational bands in odd-mass nuclei. In addition, we have discussed the energy staggering in these bands, in terms of the signature splitting.

While the description of the energy spectra of these nuclei is in general very good, there is a general tendency in the model that the moment of inertia is underestimated. Having checked that changes in the mean field deformation do not induce changes in the moment of inertia in these nuclei when the PSM is employed, we could speculate that a monopole pairing strength is excessively strong and could be responsible for this effect. Modifying this interaction would have an important effect in the spectra with only minor changes in the yrast wave functions [22]. In any case, we preferred to leave the PSM parameters unchanged, i.e., use the same employed in the calculation of ^{48}Cr, to exhibit the consistence of the description for even- and odd-mass nuclei in this mass region.

Acknowledgement

V.V. is a fellow of Conacyt (Mexico). Partial financial support from Conacyt is acknowledged.

References

[1] J.A. Cameron et al., Phys. Rev. C 49 (1994) 1347.
[2] J.A. Cameron et al., Phys. Lett. B 235 (1990) 239;
J.A. Cameron et al., Phys. Lett. B 319 (1993) 58;
J.A. Cameron et al., Phys. Lett. B 387 (1996) 266.
[3] J.A. Cameron et al., Phys. Rev. C 58 (1998) 808.
[4] S.M. Lenzi et al., Phys. Rev. C 56 (1997) 1313.
[5] F. Brandolini et al., Nucl. Phys. A 642 (1998) 387.
[6] E. Caurier, A.P. Zuker, A. Poves, G. Martínez-Pinedo, Phys. Rev. C 50 (1994) 225.
[7] E. Caurier, J.L. Egido, G. Martínez-Pinedo, A. Poves, J. Retamosa, L.M. Robledo, A.P. Zuker, Phys. Rev. Lett. 75 (1995) 2466.
[8] G. Martínez-Pinedo, A. Poves, L.M. Robledo, E. Caurier, F. Nowacki, J. Retamosa, A. Zuker, Phys. Rev. C 54 (1996) R2150.
[9] G. Martínez-Pinedo, A.P. Zuker, A. Poves, E. Caurier, Phys. Rev. C 55 (1997) 187.
[10] P. Ring, P. Schuck, The Nuclear Many Body Problem, Springer-Verlag, Berlin, 1980.
[11] T. Tanaka, K. Iwasawa, F. Sakata, Phys. Rev. C 58 (1998) 2765.
[12] K. Hara, Y. Sun, T. Mizusaki, Phys. Rev. Lett. 83 (1999) 1922.
[13] K. Hara, Y. Sun, Int. J. Mod. Phys. E 4 (1995) 637.
[14] J.A. Sheikh, K. Hara, Phys. Rev. Lett. 82 (1999) 3968.
[15] T. Bengtsson, I. Ragnarsson, Nucl. Phys. A 436 (1985) 14.
[16] M. Dufour, A.P. Zuker, Phys. Rev. C 54 (1996) 1641.
[17] V. Velázquez, J. Hirsch, Y. Sun, Nucl. Phys. A. 643 (1998) 39.
[18] A. Bohr, B.R. Mottelson, Nuclear Structure, Benjamin, New York, 1975.
[19] K. Hara, Y. Sun, Nucl. Phys. A 537 (1992) 77.
[20] Y. Sun, D.H. Feng, S.X. Wen, Phys. Rev. C 50 (1994) 2351.
[21] ENSDF, http://ie.lbl.gov/ensdf/welcome.htm
[22] A.P. Zuker, J. Retamosa, A. Poves, E. Caurier, Phys. Rev. C 52 (1995) R1742.